

"Experimental analysis of the dynamic inflow effect due to coherent gusts"

Frederik Berger, Lars Neuhaus, David Onnen, Michael Hölling, Gerard Schepers, and Martin Kühn,
Wind Energ. Sci. Discuss., <https://doi.org/10.5194/wes-2022-2>, 2022

Authors response to reviewer comments

We would like to thank Georg Raimund Pirrung and one anonymous reviewer for their thorough review, time and constructive and very meaningful comments. Their input helped to improve the original manuscript.

We addressed all comments and reply to these point by point. First the comment is repeated (in italics), followed by an answer of the authors and if applicable the excerpt from the LaTeX-Diff file (framed), highlighting the changes. Line numbers in the comments refer to the discussion version and line numbers in the response to the LaTeX-Diff of the revised manuscript, which is also attached as a complete version.

Anonymous, Reviewer #1

Reviewer #1 general comments:

R1G1. **[Reviewer #1]** *The justification for modifying Oye's dynamic inflow model is weak; why do the time constants from the original model still work when you change the filter's input from the induced velocity at the rotor into the absolute velocity in the wake?*

I think you assume $u_{2,int} = u_0 - 2u_{ind,int}$ $u_{2,qs} = u_0 - 2u_{ind,qs}$ for eq (17) and eq (18). (Please explain explicitly if it's the case)

If you substitute $u_{2,int} = u_0 - 2u_{ind,int}$ $u_{2,qs} = u_0 - 2u_{ind,qs}$ into eq (17), you will get
$$u_{ind,int} + \tau_{slow} \frac{du_{ind,int}}{dt} = u_{ind,qs} + k\tau_{slow} \frac{du_{ind,qs}}{dt} + \frac{1-k}{2} \tau_{slow} \frac{du_0}{dt}$$

Basically, it's just eq (12) plus the term $\frac{1-k}{2} \tau_{slow} \frac{du_0}{dt}$, which is totally independent from the wake velocity. And the wake velocity usually is not a known variable in BEM, anyway, you need to get it based on the assumption of the quasi-steady optimal rotor as you did in this paper. Therefore, please better justify your modification and better formulate it.

[Authors] Thank you for this very helpful comment. We changed the formulation of the model as suggested by you. We further completely reworked the motivation and description of the model (also thanks to the insights gotten from this comment) and think we have made a major improvement here. We hope that the motivation now is clarified:

325 **Improved formulation of Øye model for gusts**

The motivation is that the delay function with τ_{slow} is meant to model the inertia of the wake. Considering a fast step-like increase in wind and resulting increase in induced velocity, a delay on the induced velocity would result in an overshoot of the far wake velocity, which can be expressed as $u_2 = u_0 - 2 \cdot u_{\text{ind}}$.

330 The improved formulation of the Øye model thus considers the filter function with τ_{slow} to act on the velocity in the far wake, instead of model is developed for the assumption of constant wind velocity and filters the induced velocity through two first-order differential equations. Schepers (2007) describes the dynamic inflow for a fast change in thrust alongside the reproduced Fig. 6 a as:

335 "The trailed vorticity is formed at the blade and convected downstream with the local total velocity, partly wake induced [...]. Then a change in bound vorticity (e.g. through a change in pitch angle) modifies the vorticity which is trailed into the wake. Due to the fact that the vorticity is convected with a finite velocity, the resulting wake becomes a mixture of 'old' and 'new' vorticity. Consequently the velocity induced by such wake includes a contribution from the 'old' and the 'new' situation"

340 Schepers (2007) estimates that the effect of this mixed wake is 'felt' by the rotor until it has travelled $2D$ to $4D$, before the induced velocity. With this approach unphysical velocity overshoots in has reached a new equilibrium. In Berger et al. (2021a) a relevant distance of $2D$ is estimated based on a comparison of wake measurements and dynamic turbine loads.

In Fig. 6 b a coherent gust, in this case a rapid decrease in wind velocity, is sketched as a turbulent box with only one grid point. When this box is pushed through the wind turbine above (e.g. with the inert wake due to fast gusts are prevented. The filter function with τ_{fast} , related to the fast change in trailed vorticity, is left unchanged. The improved formulation is given in Eq. mean wind velocity of the seed as is done in BEM and FVWM simulations) in Fig. (17, ??), whereas Eq. 6 (14-16) remain

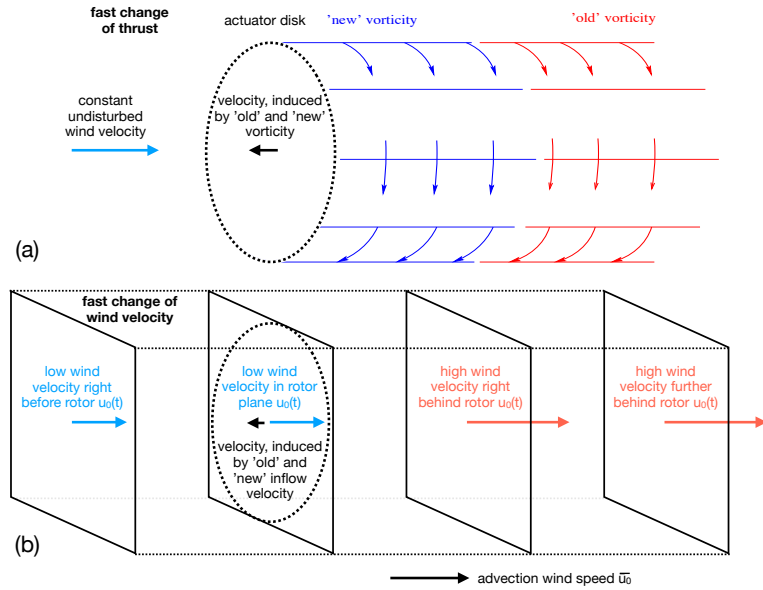


Figure 6. Wake with mixed vorticity as a result of a fast change in thrust (modified from Schepers (2007))(a) and simplified turbulent box with coherent gust like sudden drop in wind velocity (b).

unchanged:-

$$u_{2,int} + \tau_{slow} \frac{du_{2,int}}{dt} = u_{2,qs} + k \cdot \tau_{slow} \frac{du_{2,qs}}{dt}$$

$$u_{ind} + \tau_{fast} \frac{du_{ind}}{dt} = \frac{u_o - u_{2,int}}{2} = u_{ind,int}$$

350 a it also causes a change in bound vorticity that is trailed into the wake. This is covered by the original Øye model.

Instead of the However, the wake with the 'old' and 'new' vorticity is convected by the local wind velocity, partly wake induced. For the shown case, this local wind velocity in the relevant wake distance is in parts higher than in the rotor plane. The wake is convected faster than in the assumption for the Øye model. This effect is expected to increase the axial velocity as additional air volume is pulled through the rotor by the inertia of the wake. This increases the angle of attack during the step change to lower wind velocity and thus leads to a more gradual change of the turbine load.

355 change to lower wind velocity and thus leads to a more gradual change of the turbine load.

To include this effect in the dynamic inflow model an additional time derivative on the undisturbed wind velocity $u_0(t)$ is added to the computation of the intermediate induced velocity (u_{ind}) the far wake velocity (u_2) is filtered in the first step by the slow time constant τ_{slow} $u_{ind,int}(t)$ in the Øye dynamic inflow model to the right-hand side of Eq. (17). In the second step the induced velocity, is filtered by the fast time constant as before in 12), which is then written as Eq. (??). The right side of that

360 equation is the intermediate induced velocity as before, just expressed based on the intermediate far wake velocity- 17). With this extra term ($k_u \cdot \tau_{slow} \frac{du_0(t)}{dt}$) any change in wind velocity drives the time filter of $u_{ind,int}(t)$. For constant wind velocity, the extra term has no impact and the model is essentially the original Øye dynamic inflow model.

$$u_{ind,int}(t) + \tau_{slow} \frac{du_{ind,int}(t)}{dt} = u_{ind,qs}(t) + \tau_{slow} \left(k \cdot \frac{du_{ind,qs}(t)}{dt} + k_u \cdot \frac{du_0(t)}{dt} \right) \quad (17)$$

A good initial fit to the experiment was found with the slow time constant τ_{slow} and the factor $k_u = 0.2$.

R1G2. **[Reviewer #1]** The formulation of the modified dynamic inflow model is developed and tested only for one case, not verified for any other cases rather than the case used to test the model. Please add a few more verification cases to test the model's reliability. If it can not be done by wind tunnel tests, then maybe using the vortex model.

[Authors] Thank you for this comment. At the moment we do have no more suitable experimental cases for comparison. However, in App. A, two further comparison cases between the BEM simulations and FVWM are presented for validation. In the first comparison the sine frequency is once doubled and once halved. In the second comparison the stochastic wind field is used as a case with different gust amplitudes. For both comparisons the improved Øye model shows a similar performance to the here presented sine case.

Appendix A: [Additional numerical validation cases](#)

Two additional comparisons between the BEM model variants (steady, Øye and improved Øye model) are presented to demonstrate the applicability of the suggested approach for varying gust scenarios. The comparison is based on $u_{ind}(t)$ at a radius of $0.6R$.

The first comparison is designed to qualitatively relate the reaction on a *sine* gust case with three different frequencies. Therefore, the time period T of one *sine* is doubled and halved, leading to frequencies of 0.5 Hz and 2 Hz, respectively. The results are shown in Fig. A1 a and b for the BEM variants and the FVWM simulations, respectively. The steady BEM and

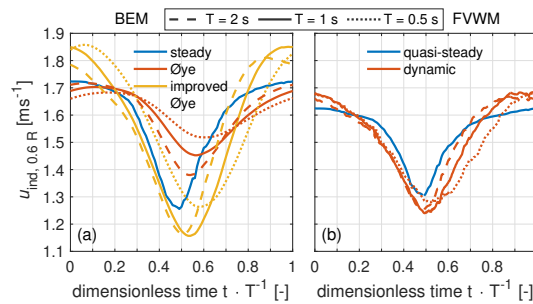


Figure A1. [Steady and dynamic induced velocity at \$0.6R\$ for the *sine* gust with variations in time periods for BEM simulation with the original and improved Øye dynamic inflow model \(a\) and FVWM simulation \(b\).](#)

quasi-steady FVWM curves as well as the solid curves at $T = 1$ s are identical to the ones on Fig. 11 d and f. These curves and the differences in the (quasi-)steady values have been discussed in the context of Fig. 11. Here the focus is on the comparison of the additional curves in relation to the dynamic curve at $T = 1$ s. For the BEM model with the Øye dynamic inflow model, $T = 2$ s leads to a larger amplitude in $u_{ind}(t)$ and $T = 0.5$ s to a reduced amplitude, as is expected. For the improved Øye model, the change to $T = 2$ s does not impact the minimum level at $0.5T$, just shifts it to a slightly earlier instance. For the maximum level these are slightly below the dynamic reference case. The same qualitative observations are made for the corresponding FVWM curve. For $T = 0.5$ s, the improved Øye model and FVWM predict similar maximum values as for their respective dynamic reference case and higher minimum values closer to the minimum values of the respective (quasi-)steady curves, but both with a time delay that is most obvious in the rise from the minimum to the maximum $u_{ind}(t)$.

The qualitative changes for doubling and halving the *sine* frequency are caught by the improved Øye model as suggested by the FVWM.

In Fig. A2 a and b a similar comparison is shown for the *stochastic* (see Fig. 8 a) wind variation, providing various gust amplitudes starting from different wind velocities.

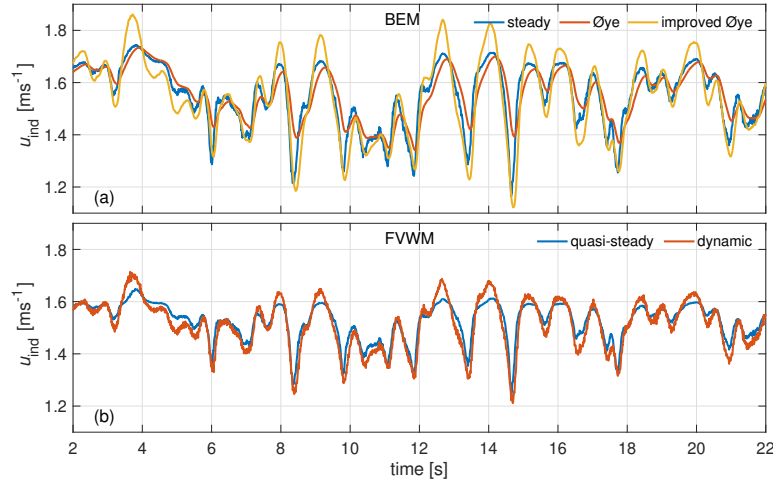


Figure A2. Steady and dynamic induced velocity at $0.6R$ for the *stochastic* gust for BEM simulation with the original and improved Øye dynamic inflow model (a) and FVWM simulation (b).

For the BEM case the original Øye dynamic inflow model gives a reduction in amplitude through the filtering approach, as is expected. The improved Øye model as well as the dynamic FVWM lead to higher amplitudes, compared to the respective (quasi-)steady cases. In general the behaviour in relation to the respective (quasi-)steady case of the improved Øye model and the FVWM are similar.

For a quantitative comparison, the difference between the (quasi-)steady and dynamic induced velocity at each time point is compared in a scatter plot in Fig. A3 a and b, where the y-axis refers to the FVWM and the x-axis to the original Øye model in Fig. A3 a and to the improved Øye model in Fig. A3 b.

Based on the Pearson correlation coefficient (ρ_{xy}), the improvements in the Øye model lead from a low negative correlation to a high positive correlation showing the good match of improved Øye and FVWM. This trend is similar for other radii. The lower y-slope ($0.47x$) is related to the mentioned general differences in amplitude of $u_{ind}(t)$ between the models.

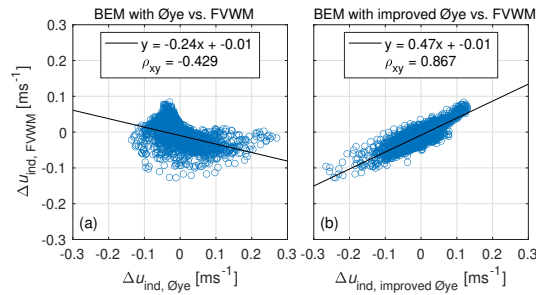


Figure A3. Scatter plot with correlation coefficients of the differences in u_{ind} between the (quasi-)steady and dynamic cases of the *stochastic* gust at $0.6R$. Comparison of FVWM and Øye in (a) and FVWM and improved Øye in (b).

R1G3. **[Reviewer #1]** From the description, the principal difference between the quasi-steady and dynamic measurement is not clear to readers.

[Authors] Thank you for this remark. You are right this information is included in the abstract but the step is missing in our description. We put the two subsections ‘Dynamic experiment’ and ‘Quasi-steady behaviour’ to subsubsections and put them under the new subsection ‘Dynamic and quasi-steady cases’. We added the following introductory paragraph:
The further additions based on the specific comments R1S36 and R1S37 are presented under these comments.

2.5 Dynamic experiment and quasi-steady cases

215 The dynamic and quasi-steady case during a gust is compared for different load and rotor flow signals. The difference between both cases results from the dynamic inflow effect. The dynamic measurement is denoted dynamic case. The quasi-steady case is the respective signal during the same gust without dynamic effects. They are interpolated from lookup-tables based on the instantaneous gust wind speed. These lookup-tables are based on a quasi-steady characterisation experiment. The processing of both the dynamic and quasi-steady signals is introduced in this subsection.

R1G4. **[Reviewer #1]** The vortex model is only used for qualitative but not quantitative comparison; why is the case? What causes the difference in quasi-steady values between the vortex model and BEM, experimental results (eg. In figure 10 a-c)?

[Authors] The vortex model was mainly added to show that the general effect of reduced load amplitudes can be caught by this type of simulation. This information then firstly is a good reassurance of the experimental results and secondly shows a way for model fine tuning in the future. The focus of the paper is on the experiment, so that we did not want to divert more from that focus than needed. However, for one case in the Appendix A now the comparison is also quantitative.

It is probably impossible to pinpoint all reasons for differences between the quasi-steady values in thrust for BEM, experiment and FVWM. However the main reason for the most obvious difference between FVWM and the other two is the differences in tip losses that are presented in Berger et al. 2020 for the high and low load case of a pitch step experiment with the same FVWM, BEM model and experimental measurement on basis of the axial induction factor. The loading of the FVWM at the tip is higher in Berger et al. 2020 and the same is seen in the simulations for this paper. The differences between experiment and BEM are quite small. Here for example also the experiment has some uncertainty as shown before, which is much larger than the difference between BEM and experiment.

The differences in u_{ind} are also partly responsible for the difference in the thrust loading. These are not influenced by tip or root effects (at the shown radius of $0.6 R$). So the differences between FVWM and BEM originate from the different modelling techniques that probably both are not perfectly right. The experiment again has a considerable uncertainty range, that covers both simulation types.

It is therefore of high importance here to carry out the comparison between dynamic and quasi-steady cases of the same experimental or simulation source, as the steady influences then are canceled out.

R1G5. **[Reviewer #1]** Labels of all the figures about experiments are confusing. They are 'quasi-steady' and 'measurement'. Does the 'quasi-steady' not stand for the quasi-steady measurement? Then why not be labeled as 'quasi-steady' and 'dynamic'?

[Authors] That is a good point. We have changed the labels as suggested to 'dynamic' to make it clearer.

R1G6. **[Reviewer #1]** Could you please include a list of Symbols?

[Authors] We have added a list of symbols in the appendix (App. B). We further simplified or removed in the text some very specific notations (e.g. $u_{0, OD, local}$) to improve the general readability.

Reviewer #1 specific comments:

R1S1. **[Reviewer #1]** p1 l2 'leads to' -not necessary, if the change rate is low

[Authors] good remark to clarify this. We changed the sentence to (ll 3-4)

of the wake. ~~For pitch actuation and fast rotor speed changes this effect leads~~ Fast changes in turbine loading due to pitch actuation or rotor speed transients lead to load overshoots. The ~~effect~~ phenomenon is suspected to be also relevant for gust

R1S2. **[Reviewer #1]** p1 l8f It's not very clear in the paper how the velocity is interpolated. Maybe explain it more explicitly

[Authors] Thank you for pointing out this imprecision. We made this more clear already here in the abstract as suggested and split the extended information into two sentences :

15 in the rotor plane during a gust situation ~~is~~ are performed. Secondly, ~~quasi-steady loads and axial velocities are interpolated from a steady characterisation experiment according to~~ corresponding quantities are linearly interpolated for the gust wind speed. ~~By comparing both cases, the influence attributed to the dynamic inflow effect is isolated. Further comparisons to from lookup-tables with steady operational points. Furthermore, simulations with~~ a typical Blade Element Momentum code

R1S3. **[Reviewer #1]** p1 l11 delete 'Based on analytical considerations'

[Authors] We reworked the abstract here and this statement was deleted (l 17)

R1S4. **[Reviewer #1]** p1 l12 'dynamic inflow effect' -what is this effect? load overshoot as you introduced above? but your observation is lower load

[Authors] You are right we should have made it more clear from the beginning that not only load overshoot can be considered as dynamic inflow effect. We have clarified this in the introduction of the effect in the abstract:

of the wake. ~~For pitch actuation and fast rotor speed changes this effect leads~~ Fast changes in turbine loading due to pitch actuation or rotor speed transients lead to load overshoots. The ~~effect-phenomenon~~ is suspected to be also relevant for gust situations, ~~however; however,~~ this was never shown. ~~The objective of the paper is to prove, and thus the actual load response is also unknown. The paper's objectives are to prove and explain~~ the dynamic inflow effect due to gusts ~~and compare, and compare and subsequently improve a typical~~ dynamic inflow engineering ~~models to corresponding measurements. A 1.8m diameter model turbine is used in the large wind tunnel of ForWind – University of Oldenburg with an active grid to impress model to the measurements. An active grid is used to impress a 1.8m diameter model turbine with~~ rotor uniform gusts ~~on the~~

R1S5. **[Reviewer #1] p1 l12 p1 l16** ‘An amplification of induced velocities’ - How does the incoming wind speed results in different induced velocity? could you explain?

[Authors] We reworked that part and made this more clear in the abstract:

~~effect due to gusts in accordance to the experiment and FVWM simulations. An amplification of induced velocities, seen in the experiment and FVWM simulation, causes the reduced load amplitudes. Therefore, classic velocities. An amplification of~~

25 induced velocities causes reduced load amplitudes. Consequently, fatigue loading would be lower. This amplification originates from wake inertia. It is influenced by the coherent gust pushed through the rotor like a turbulent box. The wake is superimposed on that coherent gust box, and thus the inertia of the wake and consequently also the flow in the rotor plane is affected.

R1S6. **[Reviewer #1] p1 l17f** ‘Therefore, classic dynamic inflow models, which filter the induced velocity, cannot predict the effect.’ -As explained in my main comments 1. the problem is not because the filtering of the induced velocity. It's because that U_0 in the original model development is assumed steady.

[Authors] Thank you for pointing this out. We have added this information and changed the sentence (and split it) to:

Contemporary dynamic inflow models ~~, which inherently assume a constant wind velocity. They~~ filter the induced velocity ~~; and thus~~ cannot predict the effect. ~~The proposed improvement to additionally consider the wake velocity for the filter of the~~

30 dynamic inflow engineering model, proves to be a straight forward but also effective modification. observed amplification of the induced velocity. The commonly used Øye engineering model predicts increased gust load amplitudes and thus higher fatigue

R1S7. **[Reviewer #1] p1 l19** ‘a straight forward’ -delete

[Authors] done

R1S8. **[Reviewer #1] p1 l19** ‘effective modification’ -We need to see more cases to conclude this

[Authors] You are right to point out that this statement with the example in the discussion paper was a bit optimistic. As discussed in R1G2 we have added additional comparison cases between Øye/improved Øye and the FVWM (as suggested by both reviewers). We have changed the sentence to match the changed model description (see R1G1) to: (ll 32-33)

loads. With an extra filter term on the quasi-steady wind velocity, the behaviour observed experimentally and numerically can be caught. In conclusion, these new experimental findings on dynamic inflow due to gusts and improvements to the Øye model

R1S9. **[Reviewer #1] p1 l21** 'fatigue' - the load caused by gust is more extreme load rather than fatigue load, no?

[Authors] The gusts that we consider in this paper are quite slow compared to the classical extreme gust cases specified in the IEC norm. The extreme operating gust (the Mexican hat) for example has a duration of 6 s. If we take this gust for the NREL 5MW turbine the model is based on and downscale the gust we would have a gust duration of $6s/70 = 0.086$ s, so 12 times faster than our wind tunnel sine gust. The dynamic inflow effect will probably also affect extreme loads, however we see the main benefit of catching these gust related lower load changes in the fatigue envelope of wind turbines at common 'gusty' conditions.

R1S10. **[Reviewer #1] p2 l34** ...Øye model '(Snel and Schepers, 1994)' -why not cite the original paper for the model?

[Authors] We added the papers Øye 1986 and Øye 1990 which lead to the model, however also kept the Snel and Schepers, 1994 reference as the model is presented here very clear and the publication is more accessible.

R1S11. **[Reviewer #1] p2 l37-46** is non-uniform inflow the focus of the paper? why do you need this paragraph?

[Authors] You are right, the focus of this paragraph can be a bit misleading. We removed the reference Perez-Becker et al. (2020) that only discusses shear and kept Boorsma et al. (2020) where also dynamic inflow effect is discussed and shifted the focus a bit more on dynamic inflow (and consequently reduced the influence of shear).

50 ~~Recently Perez-Becker et al. (2020) and Boorsma et al. (2020) compared aeroelastic simulations based on Blade Element~~
~~Momentum (BEM) theory and Free Vortex Wake Methods (FVWM).~~ In addition to the need of engineering models for dynamic
inflow effects, ~~BEM Blade Element Momentum (BEM) theory~~ is based on the assumption of axial and uniform inflow. ~~Current~~
~~BEM tools used in industry and academia have different implementations to handle non-uniform inflow (Boorsma et al., 2020)~~
~~. FVWM~~ Free Vortex Wake Methods (FVWM) on the other hand ~~models model~~ dynamic inflow effects and ~~also~~ non-uniform
55 inflow intrinsically. ~~Both investigations~~ Boorsma et al. (2020) looked at the influence of turbulent wind fields with shear on the
loading of wind turbines. ~~Both~~ They found relevant lower fatigue loading for the out-of-plane blade root bending moments and
tower bottom fore-aft bending moment for the higher fidelity FVWM type simulations. The implementations of non-uniform
inflow in BEM was identified as one ~~main-relevant~~ contribution to this behaviour ~~in both investigations. Boorsma et al. (2020).~~
~~however they~~ also suspected the dynamic inflow effect to be responsible for some of the differences between BEM and FVWM
60 in turbulent inflow.

R1S12. **[Reviewer #1] p2 l49** 'give a clear indication for' - observe

[Authors] That is a much clearer statement – we have implemented it as suggested.

R1S13. **[Reviewer #1] p2 I51** ‘a slight load overshoot for’ - Interesting! Overshoot is shown in those projects, but lower loading is observed from BEM, vortex model and experiment in the current paper. Could you explain the opposite observation?

[Authors] We specified here that ‘BEM based simulations with engineering models suggested a slight load overshoot..’. So the trend they describe in their investigation with e.g. the Øye and ECN dynamic inflow models is comparable with the trend that is presented with the (original) Øye dynamic inflow model in this paper.

R1S14. **[Reviewer #1] p3 I58** ‘prove’ - prove? throughout the document

[Authors] Thank you for pointing this out. We corrected that throughout the document.

R1S15. **[Reviewer #1] p4 I91** as ‘ n_{time}/n_{length} ’ - it will end up 3500?

[Authors] Thank you for making us aware of that (slightly embarrassing) mistake. It has to be $n_{time} * n_{length} = 0.71$. We changed this accordingly.

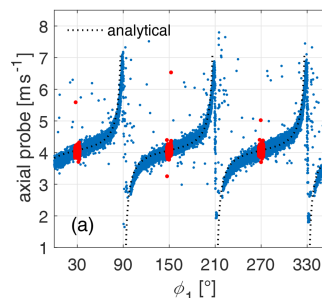
R1S16. **[Reviewer #1] p7 I153** ‘wake induction factors’ -what's the definition?

[Authors] We added a definition in a sentence after the introduction:

170 ~~used for the method and probed in the bisectrix of two blades~~ These are equal to the induction factors of a ring of an actuator disk and do not consider the induction contribution from the individual blades. The method is derived based on the theorem

R1S17. **[Reviewer #1] p7 I153f** ‘The local velocity in the rotor plane is used for the method and probed in the bisectrix of two blades.’ -the induction obtained by this method should be lower than the disc-averaged induction.

[Authors] Actually this is the core of the method that is described in Herraiez et al. 2018 and based on a derivation of the Biot-Savart law. Below is Fig. 5 a of Berger et al. 2021 that we also mention in the text (we have made this more prominent now). One can think of the signal of the axial probe over azimuth to be the sum of two signals. One is the induced velocity due to the blade induction (equal to the analytical dotted line with mean value at 0) and the other is the axial velocity as it would be present for an actuator disk (e.g. in a simulation), which is the offset to the mean value of 4 ms^{-1} here. For axial and uniform inflow and even loading of the rotor blades this undisturbed axial velocity can be directly probed from the bisectrix.



Probed axial velocity at $0.7 R$ near design conditions at $TSR 7.4$, pitch -0.9° and 6.1 ms^{-1} ; Fig. 5 in Berger et al. 2021

The method by Herráez et al. (2018) is used to derive the wake induction factors. ~~The local velocity in the rotor plane is used for the method and probed in the bisectrix of two blades~~ These are equal to the induction factors of a ring of an actuator disk and do not consider the induction contribution from the individual blades. The method is derived based on the theorem of Biot-Savart. For axial and uniform flow ~~the probed velocity is free of the influence of the bound circulation as the blade induction~~, the rotor blades have identical loading and circulation distribution at all azimuth positions. The velocity is probed in the bisectrix of two blades. Each blade's influence on the induced velocity due to its bound circulation is counterbalanced and thus cancels out. ~~Therefore the local velocity equals the radially averaged velocity in the rotor plane. For this axial and uniform flow the~~, apart from the tip and root region due to the tip and root vortex, respectively. For the main part of the blade, however Herráez et al. (2018) demonstrate the good applicability to derive the actual angle of attack distribution and thus velocity triangles at the blade segments from the measurement derived wake induction factors ~~thus are equal to the induction factors~~. The method was developed for steady operation, however, it was shown in a prior study in Berger et al. (2021a) to be also applicable to study the transient changes in induction factors, maintaining axial and uniform conditions.

therefore be interpreted with care. The application of this method ~~to MoWiTO~~ with the same 2D LDA setup ~~is introduced and discussed in more detail on MoWiTO~~ is presented in detail and validated for an axial velocity probe over all azimuth angles at operation near design conditions in Berger et al. (2021a) (Sect. 2.1.3 and App. A.). The same threshold value for the bisectrix position of the rotor azimuth angle of $\pm 3^\circ$ was applied, as this showed to be a good compromise between data samples and quality.

R1S18. **[Reviewer #1] p7 l156** 'the radially averaged velocity in the rotor plane.' -Why? it's free of the influence of the bound circulation, but it will be influenced by tip and root vorticity.

[Authors] We completely understand your confusion here. As pointed out by the 2nd reviewer (R2S2) it has to be 'azimuthally averaged' instead of 'radially averaged'. Then the statement is true (excluding the root and tip regions of course). The part however was deleted in the rework of the passage (see excerpt R1S17 l 174).

R1S19. **[Reviewer #1] p7 l156f** 'For this axial and uniform flow the wake induction factors thus are equal to the induction factors.- Why? I don't understand

[Authors] Thank you for this helpful question. For these axial and uniform flows the wake induction factors can be used to construct the velocity triangle at the blade sections as shown by Herraiez et al. 2018. Most of the time when people talk about axial induction factors, actually axial wake induction factors are meant. For example in a BEM code only these are considered and other effects like misaligned flow or dynamic stall are modelled by engineering models either directly acting on the angle of attack or building on the wake induction factors.

We have clarified that part in the text (see excerpt R1S17 ll 175-178), by referring to the fact that the angles of attack at the blade segments can be derived from these wake induction factors and so the velocity triangles, which is essentially what we need. So we have transported the key message and improved the understandability.

R1S20. **[Reviewer #1] p7 l170 typo**

[Authors] corrected

R1S21. **[Reviewer #1] p9 l186** ‘obtained from Xfoil’ -no measurement data are available as the model wind turbine is scaled based on the NREL 5MW?

[Authors] For the respective Reynolds numbers unfortunately no polar measurements are available for the SG6040 and SG6041 profiles.

R1S22. **[Reviewer #1] p9 l202** ‘we see’ - where can we see it?

[Authors] We added the reference to the respective figure in the results sections to make it more clear. (ll 231-233)

signal. As the rotational frequency of 8 Hz of the rotor is a multiple of the frequency of the *sine* at 1 Hz ~~we see there are~~ 24 data point clusters for this three bladed turbine over one *sine* period ~~-(in coming Sect. 3.2 Fig. 9 a to c)~~. This data is binned to clusters and the mean value of each bin is taken as a representative value.

R1S23. **[Reviewer #1] p10 Eq(11)** why are there two rho?

[Authors] Thank you for pointing out this mistake to us. There should of course only be one rho. We have removed one rho.

$$C_{\text{flap}} = \frac{M_{\text{flap}}}{\frac{1}{2} \rho u_0^2 \pi R^2 \frac{2}{3} R} \frac{n_b M_{\text{flap}}}{\frac{1}{2} u_0^2 \pi R^2 \frac{2}{3} R} \quad (11)$$

R1S24. **[Reviewer #1] p10 l227** ‘Figure 4. Turbine characteristics for’ -so the quasi-steady loads are interpolated from this figure? did you explain it explicitly?

[Authors] That is right. We have changed the first two sentences under the subheading ‘Quasi_steady behaviour’ in Sect. 2.6 to make the procedure clearer directly at the beginning of the section:

250 Quasi-steady behaviour

~~The quasi-steady case is based on a~~ Quasi-steady turbine loads and rotor flow are obtained based on linear interpolation from non-dimensional lookup-tables for a range of TSR and dimensionalised again. These lookup-tables are based on a detailed

R1S25. **[Reviewer #1] p11 l236** ‘TSR -what's the designed optimal TSR of this rotor?

[Authors] The design TSR is 7.5 as for the NREL 5MW turbine. We added the information in the introduction of the turbine.

The turbine is aerodynamically scaled based on the NREL 5 MW reference turbine (Jonkman et al., 2009) and maintains the design TSR (7.5), thrust and power characteristics, as well as the non-dimensional lift and thus induction distribution. The turbine blades are scaled by a geometrical factor of $n_{\text{length}} = \frac{1}{70}$. Influenced by structural constraints the time scaling of the

R1S26. **[Reviewer #1] p11 l236** ‘sine protocol’ -not for the staircase?

[Authors] We agree this statement should be clarified. We made it more clear, that it is based of course on the staircase protocol. However as can be seen in Fig 4 the *staircase* protocol also contains measurement points at TSR lower than 5.6, which are not needed for the interpolation of the quasi-steady values. (ll 268-269)

The solid lines represent the highest, lowest and middle operational TSR configurations for the needed range of the sine protocol within the case within the staircase characterisation. The errorbars indicate the quadratic error of the inflow uncertainty

R1S27. **[Reviewer #1] p12 l257** ‘shy off’ -marked

[Authors] corrected typo

R1S28. **[Reviewer #1] p12 l264** ‘leading to a load overshoot for a pitch step’ -not necessary. I think it should be dependent on the changing rate

[Authors] You are right, this is of course only true for a fast change in the rotor load. We changed the sentence accordingly:

295 In BEM simulations, engineering models are needed to catch the dynamic inflow effect. By filtering the induced velocity, the inertia of the wake is considered, leading to a load overshoot for a ~~pitch step. For constant wind velocity u_0 the axial induction a and far wake velocity u_2 show the same gradual change between two steady operational states as the induced wind velocity u_{ind} , as $u_{ind} = a \cdot u_0$ and $u_2 = u_0(1 - 2a)$, respectively. Consequently applying the filter on a or u_2 would not change the behaviour of the model, given constant u_0 .~~ sudden change in rotor load, e.g. by a fast pitch step.

R1S29. **[Reviewer #1] p12 l267f** ‘Consequently applying the filter on a or u_2 would not change the behaviour of the model, given constant u_0 ’ - marked

[Authors] This part was removed as it is not needed anymore with the new introduction of the improved Øye model.

R1S30. **[Reviewer #1] p13 l292f** ‘a delay on the induced velocity would result in an overshoot of the far wake velocity’ -why?please explain

[Authors] This part was completely reworked (see R1G1) and the mentioned statement is no longer in the text.

R1S31. **[Reviewer #1] p13 l295** ‘With this approach unphysical velocity overshoots in the inert wake due to fast gusts are prevented.’ -please explain

[Authors] This part was completely reworked (see R1G1) and the mentioned statement is no longer in the text.

R1S32. **[Reviewer #1] p14 l328** 'Fig. 6' -in Fig. 6 - 10, the legends are confusing. The quasi-steady is also from the quasi-steady measurement, right? you labeled as "quasi-steady", and 'experiment' sounds like simulation and experiment. It's better to label as "quasi-steady meas" and 'dynamic meas'

[Authors] Thank you for this comment. You are right, that quasi-steady is based on the characterization measurement. We have now labelled those as 'quasi-steady' and 'dynamic', as suggested in (R1G5)

R1S33. **[Reviewer #1] p17 l375** ' $u_{0,0.7D,mean}$ ' -what does it mean?

[Authors] It is $u_0(t)$ as shown in Fig. 6 (preprint). We deleted that statement here as it is on the one hand a bit confusing and does not add real information. The plateau is indicated by the uncertainty band of the quasi-steady case that is based on the uncertainty band of $u_0(t)$. Directly in $u_0(t)$ this plateau is not visible. That info however is implied in the comment on the uncertainty band. (ll 446-448)

0.4 R and 0.6 R , a plateau can be seen in the dynamic case around $t = 0.7$ s. This effect is also indicated in the uncertainty band of the quasi-steady case but not in the ~~global-mean- $u_{0,0.7D,mean}$~~ nor the dynamic load measurements. This indicates a local flow pattern that is smoothed out globally.

R1S34. **[Reviewer #1] p17 l377** ' u_0 -is $U0$ constant throughout the paper? If not, maybe better to write as $U0(t)$ to be clear?

[Authors] You are right, it makes it clearer to just use $u_0(t)$. We have implemented that accordingly.

In Fig. 9 d, e and f, the induced velocity ~~$u_{ind} = u_0 - u_{ax}$~~ $u_{ind}(t) = u_0(t) - u_{ax}(t)$ for the steady and dynamic case are plotted
450 for the three radii. The reference velocity for the ~~dynamic case is the corresponding local~~ steady and dynamic case are the wind

R1S35. **[Reviewer #1] p17 l400** ' $mean_{u0,0D}$ ' -marked

[Authors] This is the spatial mean wind velocity of the three reference measurements in the rotor plane

R1S36. **[Reviewer #1] p18 Fig. 8** 'quasi-steady' -I didn't get how the quasi-steady velocities are interpolated from the measurement.

[Authors] Thank you for this comment to improve the understandability of our paper. We have extended and improved the description of the method in Sect. 2.6 and hope that it is now clear.

The axial (see Eq. (1)) and tangential (see Eq. (2)) induction factors are obtained with the same *staircase* wind protocol.
265 Based on these also the angle of attack (see Eq. (3)) is obtained. ~~Three representative distributions over the~~ The lookup-tables

~~for the quasi-steady rotor flow are constructed for the nine considered radii and nine different TSR values (in TSR range 5.6 to 9.5). For clarity only three representative measured distributions over~~ radius are shown ~~for chosen TSR~~ in Fig. 5 a, b and c.

R1S37. [Reviewer #1] p19 I406 'Figure 10. Steady and' - Could you explain the difference in quasi-steady value between the FVWM and BEM, experimental data?

[Authors] The steady values for the BEM case are BEM simulations where the Øye model is disabled. For the FVWM we use a linear interpolation with the gust wind velocity from a lookup-table constructed from a staircase wind characterization for thrust and u_{ind} over wind velocity. In the experiment the thrust and u_{ind} are both (for quasi-steady and dynamic) based on the flow measurements (the thrust is reconstructed with the airfoil polars for both the quasi-steady and dynamic case). The axial and tangential induction (and consequently used to get to u_{ind} and thrust) of the quasi-steady case is interpolated by TSR from the corresponding lookup-table.

In the text we have improved the introduction how the quasi-steady cases for the experiment are constructed (see R1S24 and R1S36). Secondly we have improved and extended the description for the simulations:

Two different kinds of simulations, a BEM and a FVWM based, are used for comparison with the experimental data. For the BEM simulation the dynamic inflow engineering model ~~can be disabled~~. Quasi-steady is disabled to get the steady case. For the FVWM the quasi-steady cases are generated ~~for the FVWM simulation as for the experiment by characterisation with similar to the experiment.~~ A lookup-table with relevant quantities is generated based on a staircase wind input ~~in the respective simulation setup~~ and the quasi-steady case is obtained from linear interpolation by the respective wind field. The same airfoil

R1S38. [Reviewer #1] p21 I454 'Axial and induced' -marked

[Authors] Changed to differentiate from p16 I367 heading. (I 536)

4.2 ~~Axial and induced velocities~~ Velocities in the rotor plane in experiment

R1S39. [Reviewer #1] p23 I524 'current dynamic inflow engineering models' - You only consider one. Please specify

[Authors] That is completely true. We specified it to the Øye model (II 607-609)

We experimentally ~~proved~~ proved the dynamic inflow effect due to gusts for wind turbines. We tested if ~~current the Øye~~ dynamic inflow engineering ~~models are~~ model is able to predict the effect and proposed an improvement ~~based on analytical considerations.~~

R1S40. [Reviewer #1] p23 I525 'based on analytical consideration' - deleted

[Authors] we deleted that part as suggested. See excerpt in R1S39

R1S41. [Reviewer #1] p23 I537 'This leads to the observed reduced load amplitudes during gusts with an unchanged performance for pitch cases.' -not so relevant. change the filtering variable or change time constant, there is no much difference in effort in implementing the model, but the wake velocity is normally not available in BEM simulations.

[Authors] With the proposed changes in the formulation of the modified model this part is obsolete and we deleted it as suggested.

620 filtering, thus leading to higher fatigue loads. As an initial model to tackle the dynamic inflow effect due to gusts we proposed an improvement in the implementation of the Øye model ~~where the filter with the slow time constant acts on the wake flow rather than the induced velocity. This leads to the observed reduced load amplitudes during gusts with an unchanged performance for pitch cases.~~ adding an additional term with a time derivative filter on the wind velocity.

R1S42. **[Reviewer #1] p23 l542** ‘Comparisons between FVWM and BEM simulations’ -Why can't you do that in this work? only qualitative comparison is provided?

[Authors] We have added in the appendix two more comparison cases (motivated by the experimental cases in the paper) with the sine with changed frequency and the turbulent case, both focusing on the induced velocity and thus the aerodynamic effect. At the core this investigation is intended to be experimental and supported by simulations to show options to build on our findings. In the mentioned investigations by Perez-Becker et al. 2020 and Boorsma et al. 2020 much more focus is put on steady comparisons between the simulation models, damage equivalent loads, various realistic wind conditions (so not only completely coherent gusts) and also controlled turbines. The planned comparisons go in such a direction and should be worth of a separate paper..

Georg Raimund Pirrung, Reviewer #2

Reviewer #2 general comments:

R2G1. **[Reviewer #2]** *In general the article is very interesting, well written and shows some novel results. I didn't expect to see the observed decreased load amplitudes due to dynamic inflow effects for the sinusoidal gust, and it is nice to see that these could be reproduced with the FVW solver.*

I agree that this effect could not be reproduced by any 'conventional' dynamic inflow model that filters the induced velocity.

[Authors] Thank you very much for this positive feedback.

R2G2. **[Reviewer #2]** *As the other reviewer pointed out, the change corresponds to adding an extra term of $(1-k)/2 * t_{\text{slow}} * (du_0/dt)$ on the right hand side of Equation (12). I reach the same conclusion. This term could easily be multiplied by a tuning parameter, by the way. Essentially, through this additional term, any change in the inflow velocity will directly drive the time filter for the 'intermediate induced velocity' in the Oye model.*

[Authors] This is a very helpful comment by both reviewers. We have implemented the proposed change. On that basis we reworked the motivation and model description substantially. Please see the new model text under R1G1.

R2G3. **[Reviewer #2]** *It clearly seems to behave well compared to the measurements and FVW computations in this particular case. The issue for me is that - because I don't understand why it should be implemented like this from a 'physical' perspective - I am unsure if it will also behave well for different amplitudes, frequencies or mean wind speeds. So it would be very good if the argumentation for the modification could be made stronger, and possibly if a few additional comparisons between BEM and FVW for different frequencies, amplitudes or mean wind speeds could be added.*

[Authors] In App. A, two further comparison cases between the BEM simulations and FVWM are presented for validation. In the first comparison the sine frequency is once doubled and once halved. In the second comparison the stochastic wind field is used as a case with different gust amplitudes. For both comparisons the improved Øye model shows a similar performance to the here presented sine case. Please see the new model text under R1G2.

Reviewer #2 specific comments:

R2S1. **[Reviewer #2]** *several places: to proove -> to prove; prooved -> proved*

[Authors] corrected

R2S2. **[Reviewer #2]** *p7 l 156 radially averaged -> azimuthally averaged (I assume)?*

[Authors] You are completely right. Thank you for pointing this out to us.

R2S3. **[Reviewer #2] p 11 | 253:** 'The stall angle is estimated based on the highest lift coefficient...'. Do I understand correctly that the 'stall angle' is the maximum lift angle? Or how was it estimated?

[Authors] That is correct. We slightly changed the text to make it more clear:

285 tions show the highest radius dependent angles of attack for the low TSR setting and decrease with increasing TSR. The stall angle is estimated ~~based on~~ to be at the highest lift coefficient at 15° for the root airfoil up to $0.4R$ and at 11.5° for the airfoil

R2S4. **[Reviewer #2] 12 | 257:** shy off -> shy of

[Authors] corrected typo

R2S5. **[Reviewer #2] p 12 | 269** 'The faster time constant τ_{fast} can be attributed to the sudden change in the trailed vorticity and the slower time constant τ_{slow} to the effect of the wake inertia.' I am not sure about this formulation. As I understand it the faster time constant (with high radial dependency) is due to the trailed vorticity change close to the rotor plane. When that change in trailed vorticity is convected further downstream, it has a more 'global' effect on the whole rotor with less radial dependency and slower rate of change.

[Authors] You are right we guess, they are of course connected. Our formulation is a bit unclear here. We incorporated your suggestions:

300 The dynamic inflow effect due to a pitch step should be described by two time constants (Pirrung and Madsen, 2018; Yu et al., 2019; Berger et al., 2021a). The faster time constant τ_{fast} can be attributed to the sudden change in the trailed vorticity ~~and the slower~~ near the rotor plane and has relevant radial dependency. When that change in trailed vorticity is convected downstream with the wake it has a more global effect and slower rate of change, described by the slower time constant τ_{slow} ~~to~~ the effect of the wake inertia with little radial dependency.

R2S6. **[Reviewer #2] p 12 Equation (13):** there is a 'd' missing in the ' du_{ind}/dt ' term

[Authors] Thank you for this hint. We have corrected that.

R2S7. **[Reviewer #2] p 13 | 311** 'The second simulation environment is the FVWM model implemented in QBlade (Marten et al., 2016).' How are the gusts actually handled in QBlade? Are they superimposed instantaneously on the wind speed everywhere (including in the wake) or are they convected somehow?

[Authors] The gusts are handled as a turbulent box and moved through the rotor domain. The wake vortices are convected based on that turbulent box.

380 wake convection is obtained by forward integration with a first-order method. ~~The~~ A turbulent wind field is handled as a turbulent box that is moved through the wind turbine domain with the hub height mean wind velocity of the turbulence seed. The turbulent wind field is also used for the convection of the wake vortices. The induced velocity is influenced by the physical

R2S8. **[Reviewer #2] p 18 Figure 8:** It seems that I don't understand this figure. Shouldn't for example a crossing of the curves in plot a) (u_{ax} , $q_s=u_{ax}$, exp) be matched by a crossing in plot d) (because $u_{ind} = u_0 - u_{ax}$, and u_0 is the same in a) and d)) are they convected somehow?

[Authors] That is a good point. We use different u_0 for the quasi-steady and the dynamic case. For the dynamic case here the reference velocity is not the spatial mean velocity (measured 0.7D in front of the turbine and then shifted in time by based on cross correlation to reference measurements at 0.4R, 0.6R and 0.8R in the rotor plane) that is used in all other plots, but the local single point reference measurements (the mentioned ones at 0.4R, 0.6R and 0.8R). The reason is that the induced velocity is very sensitive to small changes in the reference velocity. The uncertainty band of the spatial mean velocity of the sine case (see e.g. Fig. 6a – preprint) indicates the spread. We found a smoother and in our eyes more realistic representation with the local reference wind velocity and opted to show that. However with the mean reference wind velocity the main trend of the increased amplitude can also be shown. We have specified that in the text and the caption of the figure:

In Fig. 9 d, e and f, the induced velocity $u_{ind} = u_0 - u_{ax}$ $u_{ind}(t) = u_0(t) - u_{ax}(t)$ for the steady and dynamic case are plotted for the three radii. The reference velocity for the ~~dynamic case is the corresponding local~~ steady and dynamic case are the wind velocity $u_0(t)$ as shown in Fig. 7 a and the corresponding local in-plane stand-still measurements ($u_{0,local}$) at the respective measurement position: measurement $u_{0,local}(t)$, respectively. The local reference velocity is used for a smoother representation of the sensitive induced velocity, as the local reference velocity also contains the described local flow patterns.

Figure 9. ~~Steady-Quasi-steady~~ and dynamic axial velocity and induced velocity for sine wind field at radii 0.4 R (a, d), 0.6 R (b, e) and 0.8 R (c, f). 95 % CI are given and errors for quasi-steady case and the induced velocity of the dynamic case were quadratically added. Note that the reference velocity for the quasi-steady and dynamic induced velocity slightly differ.

R2S9. **[Reviewer #2] p20 l 441:** 'The observed dynamic difference has a duration of about 0.3s, being twice the typical time constant for dynamic inflow phenomena'. I don't quite understand where the 0.3 comes from and how it relates to the time constants. Also I don't quite follow where the typical time constant comes from. For $a=0.33$ for example, t_{slow} in Equation 14 is almost equal to $2 R/u_0$. The time constant for dynamic inflow is generally said to be proportional to R/u_0 , but there can be a factor involved.

[Authors] Thank you for this comment. We see that this part on the one hand is a bit confusing in itself and secondly that the usage of the typical single time constant as motivated in Schepers1994 (and in general used as a scaling parameter as you pointed out) alongside the two time constant Øye model is a bit confusing. We addressed that in two parts of the paper.

At first the key message behind the first sentence you cite was to clearly show that the observed effect of reduced load amplitudes is not based on unsteady profile aerodynamics. We specified and simplified that passage to deliver this key message avoiding the reference to the typical time constant:

The ~~observed dynamic difference has dynamic and quasi-steady loads differ for~~ a duration of about 0.3s, being twice the typical time constant for dynamic inflow phenomena ($\tau_{typ} = \frac{R}{u_{0,mean}} = 0.14s$). $\Delta t = 0.3s$ between $t = 0.3s$ and $t = 0.6s$ (see Fig. 7). In contrast, time constants for unsteady aerodynamic effects on the profile level, like dynamic stall and the Theodorsen effect, range from 1 ms to 10 ms here, estimated by the ratio of chord length to relative wind velocity. The exceeding of the stall level at the root (up to 0.25 R) at the high wind velocity tipping point further does not coincide with the phase of interest of the sine gust. ~~We thus rule out~~ As Δt is at least 30-times higher than the typical time constant for unsteady aerodynamic effects on the profile level, a relevant contribution of unsteady profile aerodynamics on the observed effect can be ruled out.

Secondly, we specified why we use the typical dynamic inflow time constant for a single as motivated in Scheper1994:

thrust coefficient via the momentum balance ($C_T = 4a(a-1)$). The ~~time constant~~ reference time constant ($\tau = \frac{1}{2}\tau_{\text{typ}}$) was chosen to be half of the typical dynamic inflow value ($\tau = \frac{1}{2}\tau_{\text{typ}} = \frac{1}{2} \frac{R}{u_{0, \text{mean}}} = 0.07 \text{ s}$, see Scheepers and Snel, 1995 $\tau_{\text{typ}} = \frac{R}{u_0}$) as introduced in Scheepers and Snel (1995) for a simple evaluation of the dynamic inflow effect with a single time constant. This

$\tau = 0.07 \text{ s}$ also equals the duration of the fast pitch step in Berger et al. (2021a) with MoWiTO, thus giving a relateable time frame for a change in turbine loading that can lead to a clear dynamic inflow effect with this similar MoWiTO setup. The typical time constant is also commonly used as a scaling parameter in two time constant dynamic inflow models as can be seen in Eq. (14). With the difference in induced velocity $\Delta u_{\text{ind}}(t) = u_{\text{ind}}(t) - u_{\text{ind}}(t - \tau)$ the difference quotient is $\frac{\Delta u_{\text{ind}}}{\tau} \frac{\Delta u_{\text{ind}}(t)}{\Delta u_0}$.

R2S10. **[Reviewer #2] p 21 l 465:** 'The reconstructed steady thrust based on these axial velocity measurements (see Sect. 2.4) shows a good match to the one based on the strain gauge measurement.' Are you talking about comparing Figure 9 and Figure 6? Please add the references to those figures.

[Authors] It is like you describe. We added the figure references as suggested as this clearly improves readability – thank you. (ll 547-548)

The reconstructed steady thrust (see Fig. 10) based on these axial velocity measurements (see Sect. 2.4) shows a good match to the one based on the strain gauge measurement (see Fig. 7). The slight differences in the absolute levels at the tipping